Neuroscience

UPR^{ER}–immunity axis acts as physiological food evaluation system that promotes aversion behavior in sensing low-quality food

Pengfei Liu, Xinyi Liu, Bin Qi

Center for Life Sciences, School of Life Sciences, Yunnan Key Laboratory of Cell Metabolism and Diseases, State Key Laboratory of Conservation and Utilization of Bio-resources in Yunnan, Yunnan University, Southwest United Graduate School, Kunming, China

Reviewed Preprint

Published from the original preprint after peer review and assessment by eLife.

About eLife's process

Reviewed preprint version 1
January 23, 2024 (this version)

Posted to preprint server
November 12, 2023

Sent for peer review
November 10, 2023

Abstract

Summary

To survive in challenging environments, animals must develop a system to assess food quality and adjust their feeding behavior accordingly. However, the mechanisms that regulate this chronic physiological food evaluation system, which monitors specific nutrients from ingested food and influences food-response behavior, are still not fully understood. Here, we established a low-quality food evaluation assay system and found that heat-killed *E. coli* (HK-*E. coli*), a low sugar food, triggers cellular UPR^{ER} and immune response. This encourages animals to avoid low-quality food. The physiological system for evaluating low-quality food depends on the UPR^{ER} (IRE-1/XBP-1) - Innate immunity (PMK-1/p38 MAPK) axis, particularly its neuronal function, which subsequently regulates feeding behaviors. Moreover, animals can adapt to a low-quality food environment through sugar supplementation, which inhibits the UPR^{ER}-PMK-1 regulated stress response by increasing vitamin C biosynthesis. This study reveals the role of the cellular stress response pathway as physiological food evaluation system for assessing nutritional deficiencies in food, thereby enhancing survival in nature environments.

eLife assessment

This **important** study presents interesting findings that suggest that the UPR and immune regulators can act as evaluators of nutritional quality in C. elegans. **Convincing** evidence expands our understanding both of physiological food evaluation systems and of the known roles of stress response pathways in organismal physiology. However, there is limited mechanistic exploration in the study, and in some cases, the effect size is small and statistical significance questionable.

Introduction

Food is essential for the survival, growth and fitness of all animals. To adapt to fluctuating environments with a wide range of food sources, animals have developed a food evaluation system. This system enables them to identify nutrient-rich food and avoids low-quality or toxic food, thereby maximizing their survival prospects [1–3]. Various sensory neuron evaluation systems in animals has evolved to evaluate food quality through vision [4,5], olfactory [3,6–12] and gustatory senses [13–15]. Besides these sensory systems that facilitate quick feeding decisions, animals may also initiate cellular stress response programs to detect nutrition/toxin and trigger food response behaviors [16,17]. This could be one of physiological food quality evaluation systems that monitor the nutritional status of consumed food. However, the signaling events in cellular stress responses involved in evaluating of specific nutrients and the mechanisms that connect these signaling activities to food behaviors are largely unexplored. More specifically, while cellular stress response through UPR^{ER} [18] and PMK-1/p38 MAPK [19] dependent immunity in response to pathogens have been extensively studied, the functions of these cellular stress response in sensing and evaluating specific nutrients from food remain unclear.

Vitamin C is an essential micronutrient that cannot be synthesized by humans due to the loss of a key enzyme in the biosynthetic pathway [20]. Animals obtain Vitamin C from their diet and possibly also from gut microbes [21]. Vitamin C is an important physiological antioxidant and a cofactor for a family of biosynthetic and gene regulatory monooxygenase and dioxygenase enzymes. It is also required for the biosynthesis of collagen, L-carnitine, and certain neurotransmitters [22,23]. Vitamin C has been associated with various human diseases including scurvy, immune defect and cardiovascular disease [20]. Therefore, food evaluation systems in animals for sensing Vitamin C could be critical for their fitness in nature. However, the role of the cellular stress response pathway as food evaluation system for sensing and evaluating Vitamin C remains unexplored.

In this study, using the low-quality food evaluation assay system we established [24], we uncovered the mechanism of cellular stress responses pathway as physiological food evaluation system in evaluating D-Glucose deficiency in food and downstream Vitamin C content in animals through the UPR^{ER} (IRE-1/XBP-1) - Innate immunity (PMK-1 p38 MAPK) axis. This mechanism promotes animals to leave low-quality food and is critical for their survival in nature environments.

Results

Low-quality food induces stress response in animals

Our previous studies have shown that Heat-killed *E. coli* (HK-*E. coli*), which lacks certain molecules, is considered a low-quality food that is unable to support animal growth [24,25]. Morevoer, through metabolic-seq analysis, we identified significant changes in a large numbers of metabolites (**Figure S1A**, Table S1), including lipids (**Figure S1B**, Table S1), amino acid and their metabolites (**Figure S1C**, Table S1), as well as coenzymes and vitamins (**Figure S1D**, Table S1). Interestingly, we observed a significant decrease in carboxylic acids and their derivatives (**Figure S1E**, Table S1) in *E. coli* after being heat-killed (**Figure S1F**, Table S1). This suggests that HK-*E. coli* is nutritionally deficient for *C. elegnas* when compared to normal *E. coli* food.

Next, we conducted two behavior assays to facilitate the analysis of the food evaluation process in animals by seeding L1 animals in assay plates (**Figure 1A** and **1B**). In the avoidance assay, wild-type animals avoided the HK-*E. coli* food (**Figure 1A**). Interestingly, in the food choice assay, animals initially showed no preference between the two types of food (1-2h), but eventually exhibited a preference for high-quality food (Live *E. coli*) up until the17h mark (**Figure 1B**, **Figure S1H**). This suggests that worms depart from the HK-*E. coli* after recognizing it as low-quality food source through ingestion.

In order to investigate the pathways in animals that response to HK-*E. coli*, we performed transcriptomics analysis on worms that were cultured with both HK-*E. coli* and Live *E. coli*. Gene-expression profiling revealed that stress response genes, including those related to biotic stimulus, immune response and response to stress, are up-regulated in animals fed with HK-*E. coli* (**Figure 1C**, Table S2). Among these up-regulated genes, we identified 11 out of 62 of UPR^{ER} target genes (**Figure 1D**, **Figure S1G** and Table S2). Additionally, about 50%-80% of up-regulated genes overlap with genes responding pathogenic bacteria [26,27] (**Figure 1E**, Table S2), suggesting that UPR^{ER} and immune pathways may responded to low-quality food. Consistent with the results of the RNA sequencing (RNA-seq) analysis, the UPR^{ER} reporter (*Phsp-4::GFP*) and immunity reporter (*Pirg-5::GFP*) were strongly induced under HK-*E. coli* feeding condition (**Figure 1F** and **1G**). Moreover, UPR^{Mt} reporter (*Phsp-6::GFP*) was weakly induced under HK-*E. coli* feeding condition (**Figure S1I**), and starved worm did not induce UPR^{ER} and immunity (**Figure S1J** and **S1K**).

Together, these findings suggest that low-quality food (HK-*E. coli*) triggers a stress response pathway in animals, including UPR^{ER} and innate immune. This implies that animals may assess the quality of food through UPR^{ER} and innate immune pathway.

Animals evaluate food quality through UPR^{ER}-immune depended physiological food quality evaluation system

To determine whether the UPR^{ER} and innate immune pathways play a role in evaluating low-quality food, we first examined whether the activation of the UPR^{ER} by HK-*E. coli* was dependent on the known signaling components of the UPR^{ER} branches, including IRE/XBP-1, PERK/ATF-4 and ATF-6 [28,29]. We observed no difference in *Phsp-4::GFP* induction with *atf-4* (**Figure S2A** and **S2J**) or *atf-6* (**Figure S2B** and **S2J**) RNAi-mediated knockdown in animals fed with HK-*E. coli*. However, knockdown of *ire-1/xbp-1* or mutation of *xbp-1* reduced GFP fluorescence (**Figure 2A, 2B** and **S2J**). Among the 11 deferentially expressed UPR^{ER} target genes in animals fed with HK-*E. coli* from RNA-seq (**Figure 1D**), 64% of the genes are IRE-mediated genes (**Figure S1G**, Table S2). The mRNA level of IRE-1-mediated splicing of *xbp-1* is also induced in animals fed with HK-*E. coli* (**Figure S2C**). These data suggest that activation of the UPR^{ER} by low-quality food depends on the IRE-1/XBP-1.

To further analyze whether XBP-1-dependent UPR^{ER} activation is critical for animals to leave low-quality food, we tested food avoidance behavior using *xbp-1* mutant. The results show that *xbp-1* mutants had a significantly decreased likelihood of leaving of HK-*E. coli*, which was rescued by expressing *xbp-1* in neuron rather than intestine (**Figure 2C**). This indicats that XBP-1-dependent UPR^{ER} activation in neuron is critical for animals to evaluate low-quality food.

We then investigated which innate immune pathway is involved in evaluating low-quality food. First, we analyzed HK-*E. coli* induced genes from RNA-seq. Among these up-regulated genes, 82 out of 409 of PMK-1-dependent genes [30] were identified (**Figure S2D**, Table S2). Second, we confirmed the induction of several well-known PMK-1 target genes in RNA-seq data[31] (**Figure S2E**) and reporter analysis (**Figure S2F** and **S2G**). Moreover, the induction of *Pirg-5::GFP* was abolished in *pmk-1* knockdown animals fed with HK-*E. coli* (**Figure 2D** and **S2K**). Third, we found that the phosphorylated PMK-1 (p-PMK-1) level was prominently increased in wild-type

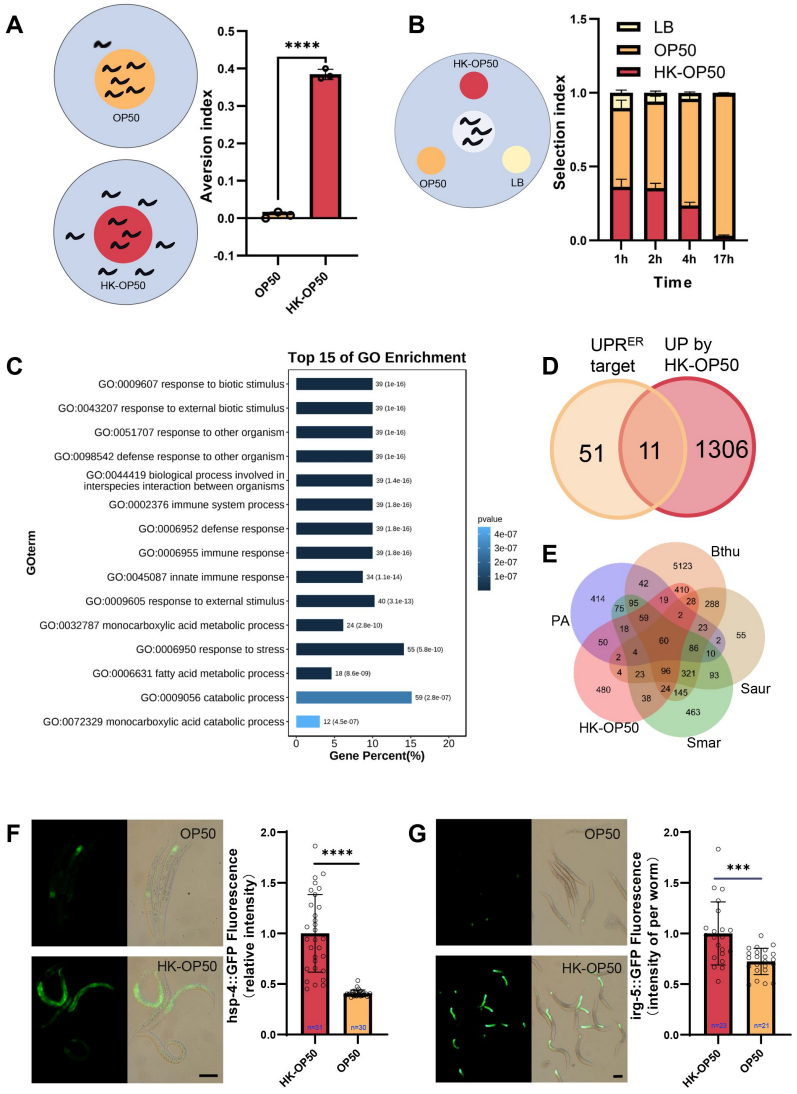

Figure 1.

The stress response is induced in animals fed low-quality food, HK-*E. coli*.

(A) Schematic drawing and quantitative data of the food aversion assay. Circles indicate the food spot for live (yellow) and HK-OP50 (red) bacteria, respectively. The animals were scored 16-17 hours after L1 worms were placed on the food spot. Data are represented as mean ±SD from three independent experiments, 79-129 animals/assay.
(B) Schematic method and quantitative data of the food selection assay. Live (yellow), heat-killed (red) *E. coli* and LB as the buffer for *E. coli* were placed on indicated position. Synchronized L1 worms were place in the center spot. The selection index was calculated at the indicated time. Data are represented as mean ±SD from eight independent experiments, 123-792 animals/assay.
(C) GO enrichment analysis of up-regulated genes in animals fed with HK-*E. coli* vs live *E. coli*.
(D) Venn diagram showing numbers of UPR^{ER} target genes and up-regulated genes in animals fed HK-*E. coli*, and their overlap.
(E) Venn diagram showing numbers of induction genes by four pathogenic bacteria and HK-*E. coli* induced genes, and their overlap. The gene expression data was extracted from published data of animals' infection with Pseudomonas aeruginosa (PA) [26], Bacillus thuringiensis (Bthu) [27], Staphylococcus aureus (Saur) [27], and Serratia marcescens (Smar) [27].
(F-G) GFP fluorescence images and bar graph showing that *Phsp-4::GFP* (F) and *Pirg-5::GFP* (G) were induced in animals fed wiht HK-*E. coli.* n is the number of worms scored from at least three independent experiments. Data are represented as mean ± SD.
For all panels, Scale bar shows on indicated figures, 50 μm. * p<0.05, ** p<0.01, *** p < 0.001, **** p<0.0001, ns: no significant difference. Precise P values are provided in Raw Data.

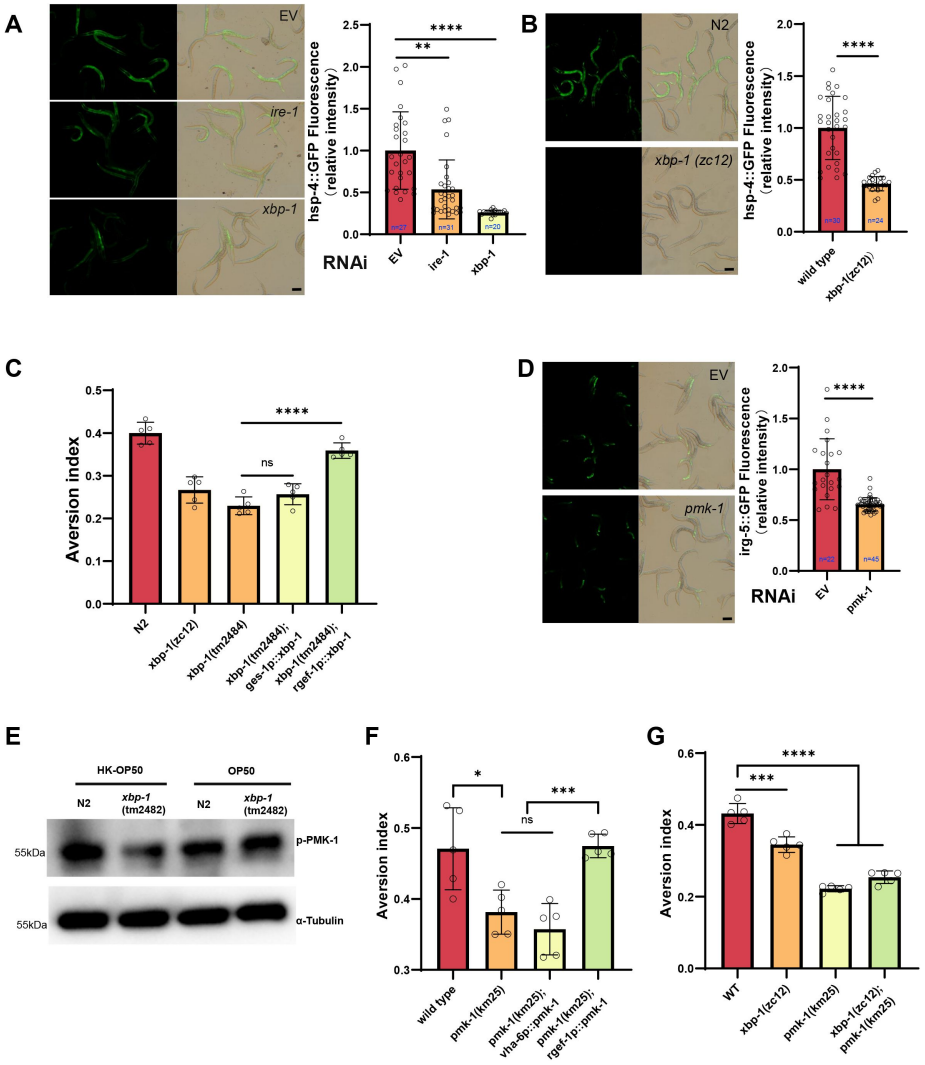

Figure 2.

Animals evaluate food quality through UPRER (ire-1/xbp-1) - Innate immunity (pmk-1 MAPK) axis.

(A-B) GFP fluorescence images and bar graph showing that HK-*E. coli* induced *Phsp-4::GFP* was decreased in animals with *ire-1* or *xbp-1* RNAi treatment (A) or *xbp-1* mutation (B). n is the number of worms scored from at least three independent experiments. Data are represented as mean ± SD.

(C) Food aversion assay showing that *xbp-1* mutation eliminated the discrimination against HK-*E. coli.* However, this effect is rescued by expressing *xbp-1* in neurons rather than intestine. Data are represented as mean ±SD from five independent experiments, 156-763 animals/assay.

(D) GFP fluorescence images and bar graph showing that HK-*E. coli* induced *Pirg-5::GFP* was decreased in animals with *pmk-1* RNAi treatment. n is the number of worms scored from at least three independent experiments. Data are represented as mean ± SD.

(E) Western blot images showing the level of p-PMK-1 in L1 animals (Wild-type N2 and *xpb-1* mutant) fed with OP50 or HK-OP50 for 4 h. The level of p-PMK-1 is induced in animals fed HK-OP50.

(F) Food aversion assay showing that *pmk-1* mutation eliminated the discrimination against HK-*E. coli.* However, this effect is rescued by expressing *pmk-1* in neurons rather than intestine. Data are represented as mean ±SD from five independent experiments, 168-492 animals/assay.

(G) Food aversion assay in wild-type, *xbp-1*, *pmk-1* and double mutant. Data are represented as mean ±SD from five independent experiments, 259-490 animals/assay..

For all panels, Scale bar shows on indicated figures, 50 μm. * p<0.05, ** p<0.01, *** p < 0.001, **** p<0.0001, ns: no significant difference. Precise P values are provided in Raw Data.

N2 animals fed HK-*E. coli* compared to feeding *E. coli* OP50 (**Figure 2E**). Finally, *pmk-1* mutants had a decreased likelihood of leaving of HK-*E. coli*, which was rescued by expressing *pmk-1* in neurons rather than intestine (**Figure 2F**). These data suggest that PMK-1 regulated immune pathway evaluates low-quality food, especially the neuronal PMK-1 has a critical function for food quality response.

XBP-1 and PMK-1 are in the same pathway for evaluating food quality

Next, we explored the connection between UPR^{ER} (IRE-1/XBP-1) and innate immunity (PMK-1 p38 MAPK) in food quality evaluation. We found that *Pirg-5::GFP* induction (**Figure S2H** and **S2K**) and PMK-1 activation (**Figure 2E**) were decreased in animals with *xbp-1* mutation or knockdown when fed with HK-*E. coli*, suggesting that XBP-1 could regulate PMK-1 under this condition. Additionally, *Phsp-4::GFP* induction under HK-*E. coli was* not affected in animals with *pmk-1* RNAi (**Figure S2I**), indicating that XBP-1-dependent UPR^{ER} activation is not regulated by PMK-1. Finally, we constructed a double mutant of *xbp-1* and *pmk-1* and found that the food avoidance phenotype of the double mutant was similar to the *pmk-1* mutant (**Figure 2G**), indicating that PMK-1 is downstream of XPB-1 in responding to low-quality food.

Sugar deficiency in HK-*E. coli* food induces stress response and avoidance behavior in animals

We then investigated which nutrients/metabolites are sensed by animals through the XBP-1-PMK-1 axis for food quality evaluation. First, we hypothesized that the nutrition status is improved in *E. coli* mutant (HK-treatment), which could inhibit URP^{ER} and immune response in animals (**Figure S3A**). We established a system for screening the *E. coli* mutant keio library (**Figure S3A**), and identified 20 *E. coli* mutants that did not induce *hsp-4::GFP* through the UPR^{ER} reporter (*irg-5::GFP*) after three rounds of screening (Table S3). From these 20 E. coli mutant, we identified 9 *E. coli* mutants that did not induce *irg-5::GFP* through the immunity reporter (*irg-5::GFP*) screening (**Figure S3B, S3C**, Table S3). Animals fed HK-*yfbR*, which catalyzes carbohydrate derivative metabolic process[32], had a decreased ability to leave food (**Figure 3A**, Table S3), indicating that HK-*yfbR* may be a higher quality food for animals compared to HK-K12.

Secondly, we preformed a metabolomics analysis of different quality food (HK-K12, HK-*yfbR* and Live-K12). We found that the level of 13 metabolites were similar between HK-*yfbR* and Live-K12, but significantly changed in HK-K12 (**Figure 3B**, **Figure S3D**, and Table S1). We also found that genes involved in glycolysis/gluconeogenesis were up-regulated in animals fed with HK-*E. coli* (**Figure S3E**), suggesting that glycolysis/gluconeogenesis metabolism is disordered in animals fed with HK-*E. coli,* which may result from changes in sugar/carbohydrate intake. The carbohydrates (D-trehalose, Lactose, and D-(+)-sucrose) were also decreased in HK-*E. coli* (**Figure 3B**), suggesting that carbohydrate deficiency may induce stress response and avoidance behavior in animals.

Thirdly, to determine which carbohydrate inhibits stress response in animals, we supplemented each metabolite to HK-*E. coli* and found that only Lactose, and D-(+)-sucrose inhibited HK-*E. coli* induced UPR^{ER} (**Figure 3C** and **3D**, **Figure S3F**). Moreover, we found from our metabolomic data that the sugar level, including Lactose, and D-(+)-sucrose, and D-(+)-Glucose, was also decreased in HK-*E. coli* (**Figure 3B**, Table S1). Since Lactose and D-(+)-sucrose are hydrolyzed to produce glucose[33,34], we wondered whether glucose also inhibits the stress response in animals. We found that D-(+)-Glucose supplementation also inhibited HK-*E. coli* induced UPR^{ER} (**Figure 3E**), immune response (**Figure 3F, 3G** and **Figure S3G**) and avoidance (**Figure 3H**). Moreover, sugar supplementation did not affect UPR^{ER} and immunity in normal food (OP50) or starved condition (NGM) (**Figure S3H** and **S3I**).

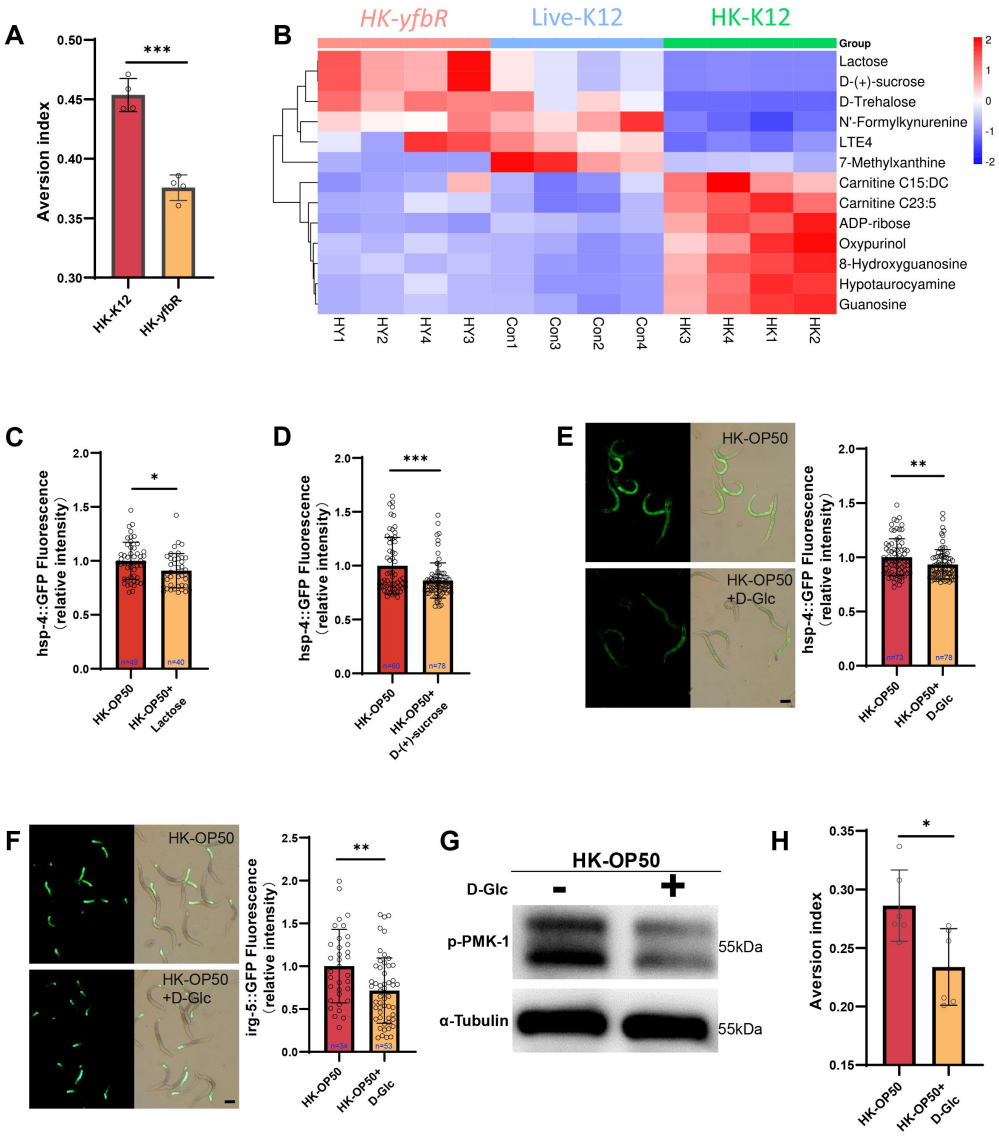

Figure 3.

HK-E. coli is low sugar food, which induce stress response and avoidance behavior in animals.

(A) Food aversion assay showing that wild-type animals eliminated the discrimination against HK-*E. coli* when *yfbR* is mutated in *E. coli*. Data are represented as mean ±SD four independent experiments, 251-490 animals/assay.
(B) Heat map showing the thirteen differential metabolites from HK-K12, HK-*yfbR*, and K12 in 4 independent experiments. Color indicates the relative level of each metabolite.
(C-D) The bar graph showing that HK-*E. coli* induced *Phsp-4::GFP* was decreased in animals with lactose (C) or D-(+)-sucrose (D) supplementation. n is the number of worms scored from at least three independent experiments. Data are represented as mean ± SD.
(E-F) GFP fluorescence images and bar graph showing that HK-*E. coli* induced *Phsp-4::GFP* (E) and *Pirg-5::GFP* (F) were decreased in animals with D-(+)-Glucose (D-Glc) supplementation. n is the number of worms scored from at least three independent experiments. Data are represented as mean ± SD.
(G) Western blot images showing the level of p-PMK-1 in L1 animals fed HK-*E. coli* with or without D-(+)-Glucose (D-Glc) supplementation for 4 h. The level of p-PMK-1 is decreased in animals fed HK-OP50+D-Glc.
(H) Food aversion assay showing that wild-type animals eliminated the discrimination against HK-*E. coli* with D-Glc supplementation. Data are represented as mean ±SD six independent experiments, 190-492 animals/assay.
For all panels, Scale bar shows on indicated figures, 50 μm. * p<0.05, ** p<0.01, *** p < 0.001, **** p<0.0001, ns: no significant difference. Precise P values are provided in Raw Data.

Together, these findings suggest that sugar/carbohydrates deficiency in HK-*E. coli* induces a stress response and avoidance behavior in animals, which can be inhibited by D-(+)-Glucose supplementation. This implies that animals may evaluate the sugars deficiency through the activation of UPR^{ER} and immune responses.

Animals could overcome a low-quality food environment by sugar supplementation through vitamin C biosynthesis

We discovered that D-(+)-Glucose supplementation inhibited HK-*E. coli* induced UPR^{ER} (**Figure 3E**), immune response (**Figure 3F, 3G** and **Figure S3G**) and avoidance (**Figure 3H**). Simultaneously, vitamin C (VC), which is synthesized by glucuronate pathway using D-Glucose [35,36] (**Figure 4A**), was found contribute to neuroprotective[37,38], immune defense[39,40], and inhibits inflammatory and ER stress[41,42]. This led us to question whether the Vitamin C biosynthesis pathway is involved in evaluating low-quality food by using D-Glucose.

Firstly, we observed an increase in the vitamin C level in animals when fed with HK-yfbR (**Figure 4B**), a high carbohydrate food compared to HK-E. coli (**Figure 3B** and **Figure S1E**). However, the VC level in bacteria is same (**Figure S4A**). The VC level also increased when D-Glucose (**Figure S4B**) or D-glucuronate (D-GlcA) was added to HK-*E. coli* (**Figure 4C**), which was abolished by knocking down VC biosynthesis genes (**Figure 4C** and **S4B**). This suggests that additional of sugar supplementation promotes VC synthesis in animals fed with HK-*E. coli*.

Secondly, we hypothesized that animals could overcome a low-quality food (HK-*E. coli*) environment by inhibiting the stress response through increasing vitamin C biosynthesis. We found that VC or D-glucuronate (D-GlcA) supplementation inhibited HK-*E. coli* induced UPR^{ER} (**Figure 4D**), immune response including *irg-5/sysm-1* reporter expression (**Figure 4E** and **Figure S4C**) and p-PMK-1 (**Figure 4F** and **4G**), as well as food avoidance (**Figure 4H**).

Finally, we asked whether inhibition of stress response and avoidance by sugar supplementation depends on the vitamin C biosynthesis pathway. We found that suppression of HK-*E. coli* induced UPR^{ER} (**Figure 4I**), immune response (**Figure 4J** and **Figure S4D**) and food avoidance (**Figure 4K**) by D-GlcA/sugar supplementation was abolished in animals with RNAi of VC biosynthesis genes. Food selection behavior assays showed that D-GlcA/sugar supplementation increased the preference for heat-killed bacteria, which was also suppressed by knocking down VC biosynthesis genes (**Figure S4E**). However, VC supplementation still suppressed the UPR^{ER} (**Figure 4I**), immune response (**Figure 4J** and **Figure S4D**) and food avoidance (**Figure 4K**), and increased the food preference (**Figure S4E**) in animals with or without RNAi of VC biosynthesis genes. This suggests that VC, as the final metabolite synthesized from D-Glucose, is critical for low-quality food response in animals.

Together, these data indicate that the Vitamin C biosynthesis pathway is critical for evaluating whether food is of higher quality and can be eaten by animals. It also suggests that animals could improve their VC levels to adapt to bad food environment.

Animals evaluate sugar and vitamin C through neuronal XBP-1 and PMK-1

As D-GlcA/sugar and VC supplementation suppressed HK-*E. coli* induced UPR^{ER}, immune response and food avoidance behavior, we investigated whether animals evaluate sugar and VC through XBP and PMK-1 dependent pathways. We performed a food selection behavior assay by adding D-Glc, D-GlcA or VC to the NGM, *E. coli* and HK-*E. coli* (**Figure 5A**). The food selection behavior assays revealed that supplementation with D-Glc, D-GlcA, or VC inhibits the animals' choice of sugar or VC on *E. coli*-OP50 feeding conditons (**Figure S4F**). This suggests that supplementation

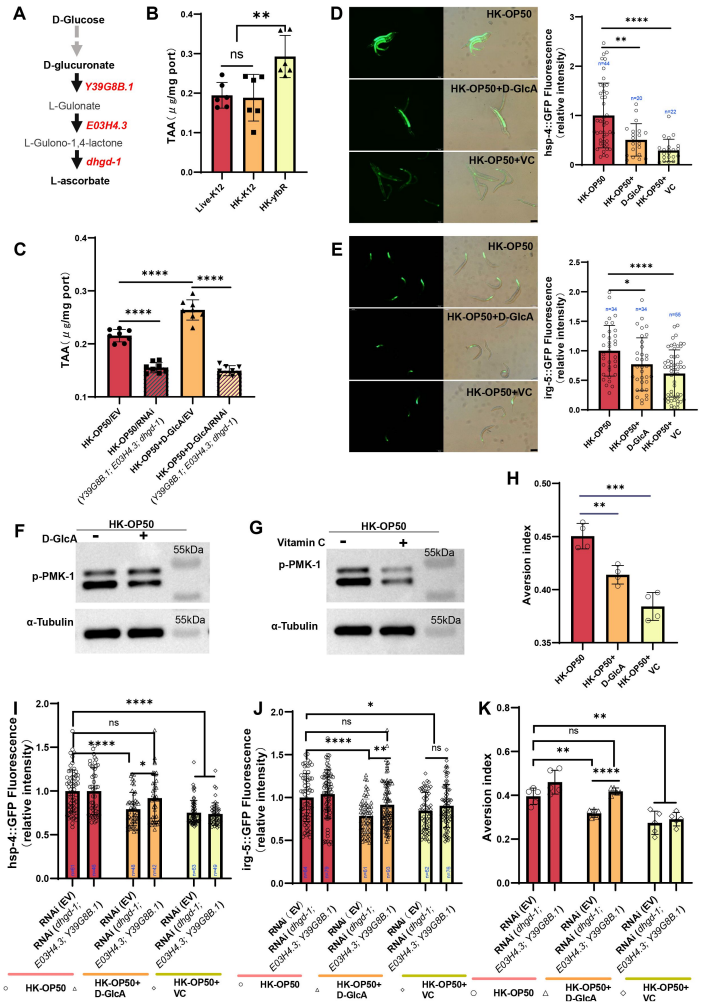

Figure 4.

Vitamin C biosynthesis pathway is critically involved in evaluating sugar in the food

(A) Cartoon illustration of a simplified, Vitamin C biosynthesis pathway in *C. elegans*. The relevant coding genes of enzymes was labeled with red.
(B) The level of total L-ascorbic acid (TAA) in animals fed with Live-K12, HK-K12, or HK-yfbR. Data are represented as mean ±SD from six independent experiments.
(C) The level of total L-ascorbic acid (TAA) in animals (control or knockdown of Vitamin C biosynthesis genes) fed with HK-*E. coli* with or without D-glucuronate (D-GlcA) supplementation. Data are represented as mean ±SD from eight independent experiments.
(D-E) GFP fluorescence images and bar graph showing that HK-*E. coli* induced *Phsp-4::GFP* (C) and *Pirg-5::GFP* (D) were decreased in animals with D-GlcA or Vitamin C supplementation. n is the number of worms scored from at least three independent experiments. Data are represented as mean ± SD.
(F-G) Western blot images showing the level of p-PMK-1 in L1 animals fed with HK-*E. coli* with D-GlcA or Vitamin C supplementation for 4 h. The level of p-PMK-1 is decreased in animals with D-GlcA (F) or Vitamin C (G) supplementation.
(H) Food aversion assay showing that wild-type animals eliminated the discrimination against HK-*E. coli* with D-GlcA or Vitamin C supplementation. N is number of independent experiments. Data are represented as mean ±SD from four independent experiments, 153-292 animals/assay.
(I-K) The bar graph showing that suppression of HK-*E. coli* induced *Phsp-4::GFP* (I), *Pirg-5::GFP* (J) and food avoidance (K) by D-GlcA supplementation was abolished in animals with RNAi of VC biosynthesis genes, which was not affect by Vitamin C supplementation. n is the number of worms scored from at least three independent experiments and Data are represented as mean ±SD(I-J). Data are represented as mean ±SD from five independent experiments, 252-537 animals/assay (K).
For all panels, Scale bar shows on indicated figures, 50 μm. * p<0.05, ** p<0.01, *** p < 0.001, **** p<0.0001, ns: no significant difference. Precise P values are provided in Raw Data.

with D-Glc, D-GlcA, or VC may alter the metabolites of live bacteria, leading to avoidance by the animals. There was no preference observed on NGM (no food condition) supplementation with D-Glc and VC (**Figure S4G**), indicating that the intake of sugar or VC alone does not influence animal preference. However, alone D-GlcA could influence worm physiology which induces preference change (**Figure S4G**). Interestingly, D-Glc and D-GlcA (**Figure 5B** and **5C**) or VC (**Figure 5D**) supplementation increased the preference for heat-killed bacteria, which was suppressed in *xbp-1* or *pmk-1* mutant animals. However, this preference was also rescued in *xbp-1* or *pmk-1* mutant animals by expressing XBP-1 or PMK-1 in neurons rather than intestine (**Figure 5B-D**), indicating that neuronal XBP-1 and PMK-1 are critical for physiological food elevation system for monitoring the level of sugar and VC under low-quality food condition.

Discussion

To better survive, animals must evolve a system to recognize and evaluate the quality of their food. This includes the sensory neuron evaluation system for immediate response and feeding decision [2], as well as physiological food evaluation system for chronic response to ingested food. In our previous study, we discovered that the TORC1-ELT-2 pathway, acting as master regulators in intestine, evaluates vitamin B2 deficiency in low-quality food (HK-*E. coli)* and regulates gut digestive activity to impact animal's food behavior [24]. To further identified the mechanism by which animals evaluate low-quality food (HK-*E. coli*), we performed metabolomics and transcriptomics analyses to identify specific nutrition deficiencies in low-quality food and the cellular response pathways that are involved in food evaluation pathway. This study identified a physiological food evaluation mechanism by which animals detect sugar (in food) and vitamin C (in animals) deficiency through UPR^{ER} (IRE-1/XBP-1) - Innate immunity (PMK-1/p38 MAPK) regulated cellular stress response program in neurons that dictates food avoidance and selection behaviors.

Unlike the sensory neuron evaluation system, which permits rapid feeding decisions through smell and taste, the cellular stress response as physiological food evaluation system describe here requires a slow and multi-step signal transduction process after the ingestion of food. The disruption of cellular homeostasis by ingested of low-quality or toxic food can activate stress response mechanisms that both increase the cellular ability to withstand and adapt to this disruption of homeostasis and promote behavioral strategies to avoid these conditions and lessen their impact on the organism. These cellular stress response mechanisms include heat shock response, unfolded protein response, oxidative stress response [43]. Therefore, this slow physiological food evaluation system is an evolutionary adaptation mechanism for detecting nutrition deficiencies in food that was not detected by quick sensory neuronal system.

One of cellular stress response, UPR^{ER}, is activated by stresses such as infection and nutrition deficiency that affect homeostasis in the endoplasmic reticulum (ER) [28]. The activation of the UPR^{ER} by expression of *xbp-1s* in the nervous system has recently been shown to promote changes in feeding and foraging behavior [44]. The p38 PMK-1 pathway regulates the expression of secreted innate immune effectors and is required for survival during infection [45]. Moreover, UPR^{ER} and innate immunity increased by disrupting in vivo state would induce worm aversion from food lawn[46–49]. Thus, these two cellular stress response pathways are critical for animals' survival in changing environment. However, whether UPR^{ER} (IRE-1/XBP-1) - Innate immunity (PMK-1/p38 MAPK) evaluates food quality under physiological conditions is largely unexplored. Our study presents evidence that low-quality food (HK-*E. coli*) activate UPR^{ER} and PMK-1, and promotes animals to leave food. It is independent of avoidance behavior of hyperactivation of kgb-1/MAPK pathway[49] (**Figure S4H**). Mover, our study also shows that neuronal UPR^{ER} and PMK-1 are critical for evaluating low-quality food. Therefore, our study established a novel physiological food evaluation system by activating the cellular stress response program with UPR^{ER} (IRE-1/XBP-1) - Innate immunity (PMK-1/p38 MAPK).

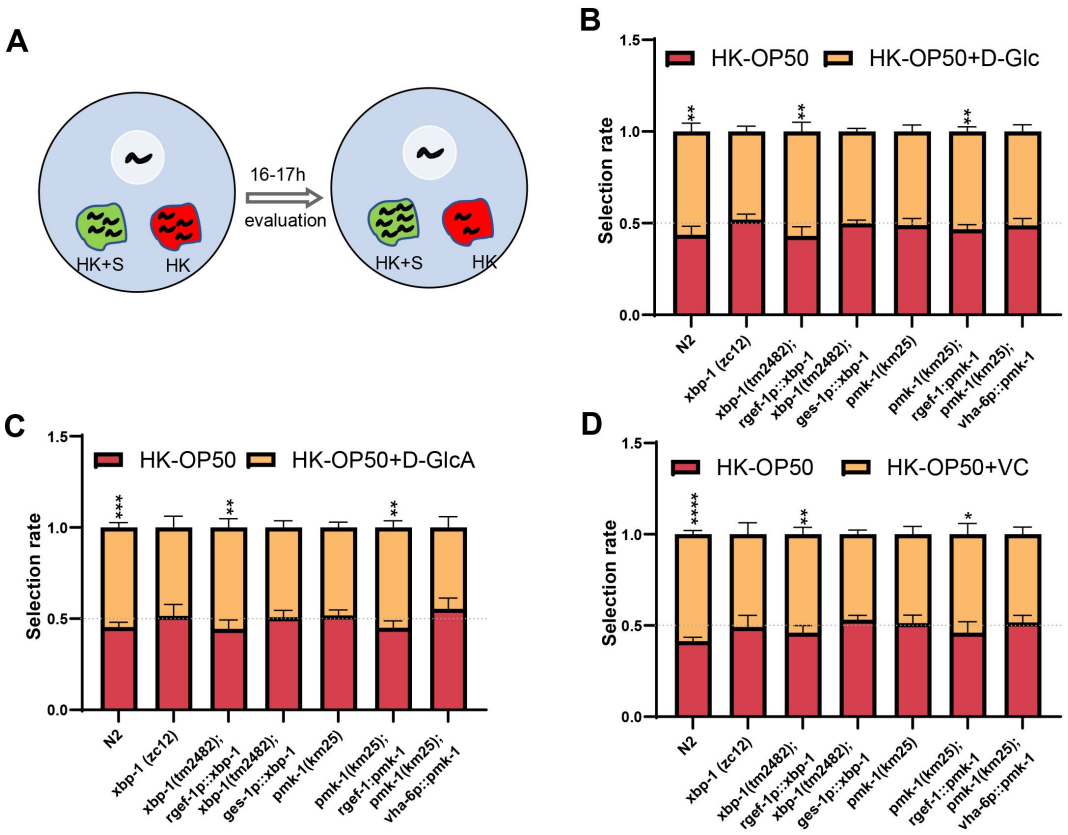

Figure 5.

Animals evaluate sugar and vitamin C through neuronal XBP-1 and PMK-1

(A) Schematic method of the food selection assay. Heat-killed *E. coli* (red) and HK-*E. coli* with chemical supplementation (green) were placed on indicated position. Synchronized L1 worms were then place in plate. After 16-17hs, the selection index was calculated.

(B-D) Food selection assay showing that *xbp-1* or *pmk-1* mutation eliminated the preference of HK-*E. coli* with D-Glc (B), D-GlcA (C) or Vitamin C (D) supplementation, which was rescued in *xbp-1* or *pmk-1* mutant animals by expressing XBP-1 or PMK-1 in neurons rather than intestine.

Data are represented as mean ±SD from five independent experiments, 68-647 animals/assay (B).

Data are represented as mean ±SD from six independent experiments, 83-701 animals/assay (C).

Data are represented as mean ±SD from six independent experiments, 67-1035 animals/assay (D).

For all panels, Scale bar shows on indicated figures, 50 μm. * p<0.05, ** p<0.01, *** p < 0.001, **** p<0.0001, ns: no significant difference. Precise P values are provided in Raw Data.

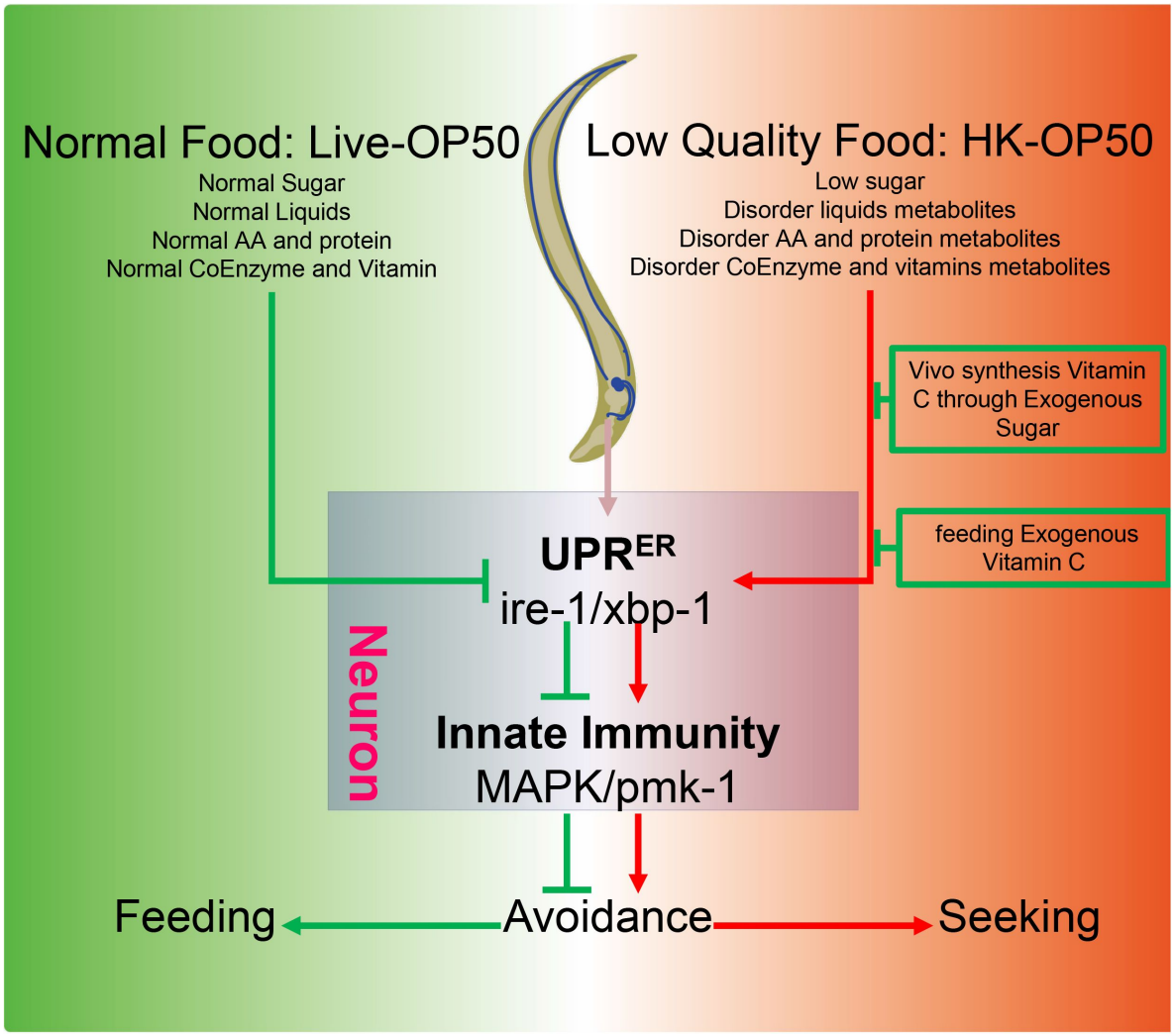

Figure 6.

Schematic model of physiological food evaluation system in evaluating/sensing sugar and vitamin C through UPR^{ER} (IRE-1/XBP-1) - Innate immunity (PMK-1/p38 MAPK) axis.

Vitamin C level is low in animals fed low sugar food, HK-*E. coli*. Sugar and Vitamin C deficiency activate cellular UPR^{ER} and immune response, which promote animals to leave low-quality food and seek better food for survival. This cellular stress regulated physiological food evaluation system depends UPR^{ER} (IRE-1/XBP-1) - Innate immunity (PMK-1/p38 MAPK) axis in neuron.

Collectively, this study uncovers the unexpected function of UPR^{ER} (IRE-1/XBP-1) - Innate immunity (PMK-1/p38 MAPK) as a physiological food evaluation system for evaluating and sensing food quality in animals. It also highlights the utility of the HK-*E. coli* (low-quality food) - *C. elegans* interaction as a means to dissect the mechanism of food evaluation system in assessing food. Most importantly, it reveals that animals are capable of altering their nutrient (Vitamin C) levels through in vivo synthesis or food intake to adapt to a poor food environment when better food choices are not available.

Author Contributions

P. L designed, performed experiments, analyzed data. X. L constructed all transgenic animals. B.Q. designed research, supervised this study, and wrote the paper with inputs from P. L.

Acknowledgements

We thank the Caenorhabditis Genetics Center (CGC) (funded by NIH P40OD010440) for strains; Dr. Zhao Shan for suggestions. This work was supported by the Ministry of Science and Technology of the People's Republic of China (2019YFA0803100,2019YFA0802100), the National Natural Science Foundation of China (32170794), Yunnan Applied Basic Research Projects (202001AV070011, 202001AW070006, 202201AT070196), the Yunnan University Startup Program.

Declaration of interests

The authors declare no competing interests.

Supplemental Figure legends

Supplemental Tables

Table S1. Metabolices analysis. Relative to **Figure S1A, S1B, S1C, S1D, S1E, S1F**, **3B**, and **S3D**.

Table S2. RNA-seq analysis. Relative to **Figure 1C, 1D, 1E**, **S1G**, and **S2D**.

Table S3. Screening data for *E. coli* mutant keio library. Relative to **Figures S3A, S3B**, and **S3C**.

Table S4. Metabolomics-seq data of HK-K12, HK-yfbR and K12.

Table S5. RNA-seq data of animals fed with HK-*E. coli OP50* and *E. coli OP50*.

Raw-data. Raw data for experiments.

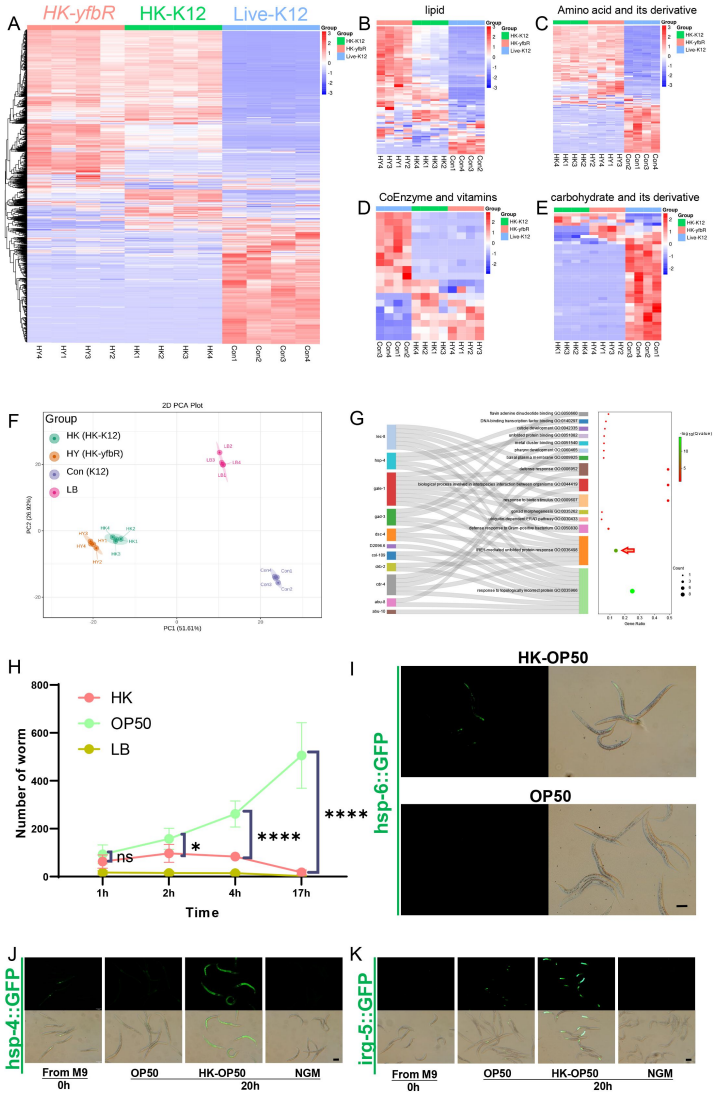

Figure S1.

Food selection assay of animals fed HK-*E. coli* or *E. coli.* Relative to Figure 1.

(A-E) Metabolomics analysis of different quality food (HK-K12, HK-*yfbR* and Live-K12). Cluster analysis of all metabolites (A), lipids and their derivatives (B), amino acids and their derivatives (C), coenzymes and vitamins (D), and carbohydrates and their derivatives (E) from Live-K12, HK-K12, and HK-yfbR.
Color indicates the relative level of each metabolite. HK-K12: heat-killed *E. coli* wild-type K12; HK-*yfbR:* heat-killed *E. coli mutant yfbR;* K12: live *E. coli* wild-type K12. z-score for standardizing data, complete for bi-clustering algorithm, and Euclidean for distance method.
(F) Principal component analysis to test the repeatability of the metabolic experiment. HK-K12: heat-killed *E. coli* wild-type K12; HK-yfbR: heat-killed *E. coli* mutant yfbR; K12: live *E. coli* wild-type K12. LB: LB buffer for culturing *E. coli*.
(G) GO enrichment analysis of UPR^{ER} dependent IRE-1 branch.
(H) The number of worms in each position calculated at the indicated time, indicating that animals initially select both foods (1-2h), but eventually favor high-quality food (Live E. coli) until 17h.
(I) UPR^{mt} Reporter (*Phsp-6:GFP*) was weakly induced in animals fed with HK-E. coli
(J) UPR^{ER} Reporter (Phsp-4:GFP) expression in animals under normal food (OP50), low quality food (HK-OP50), and starved (M9: hatching L1 worm in M9, NGM) condition;
(K) Immunity Reporter (Pirg-5:GFP) expression in animals under normal food (OP50), low quality food (HK-OP50), and starved (M9: hatching L1 worm in M9, NGM).
For all panels, Scale bar shows on indicated figures, 50 μm. * p<0.05, ** p<0.01, *** p < 0.001, **** p<0.0001, ns: no significant difference. Precise P values are provided in Raw Data.

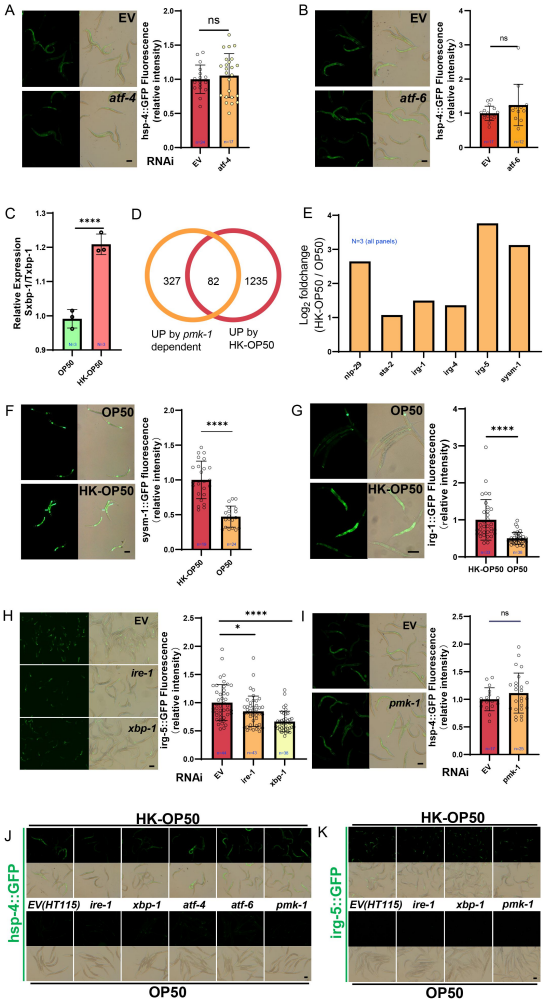

Figure S2.

UPRER and Innate immunity pathway in animals are critical for evaluating HK-*E. coli*. Relative to Figure 2.

(A-B) GFP fluorescence images and bar graph showing that HK-*E. coli* induced *Phsp-4::GFP* was not affected in animals with *atf-4* (A) or *atf-6* (B) RNAi treatment. n is the number of worms scored from at least three independent experiments. Data are represented as mean ± SD.
(C) qPCR showing that IRE-1-mediated splicing of *xbp-1* mRNA is induced in animals fed with *HK-E. coli*.
(D) Venn diagram showing the numbers of PMK-1 dependent genes [30] and up-regulated genes in animals fed HK-*E. coli,* and their overlap.
(E) The expression of PMK-1 dependent genes which was extracted from RNA-seq data from animals fed with *HK-E. coli*. The data from average of three independent experiments (N=3)
(F-G) GFP fluorescence images and bar graph showing that *Psysm-1::GFP* (F) and *Pirg-1::GFP* (G) were induced in animals fed *HK-E. coli.* n is the number of worms scored from at least three independent experiments. Data are represented as mean ± SD.
(H) GFP fluorescence images and bar graph showing that HK-*E. coli* induced *Pirg-5::GFP* was decreased in animals with *ire-1* or *xbp-1* RNAi treatment. n is the number of worms scored from at least three independent experiments. Data are represented as mean ± SD.
(I) GFP fluorescence images and bar graph showing that *Phsp-4::GFP* was not affected in animals with *pmk-1* RNAi treatment. n is the number of worms scored from at least three independent experiments. Data are represented as mean ± SD.
(J) UPR^{ER} Reporter (Phsp-4::GFP) expression in animals with candidate RNAi feeding OP50 or HK-OP50
(K) immunity Reporter (Pirg-5::GFP) expression in animals with candidate RNAi feeding OP50 or HK-OP50
For all panels, Scale bar shows on indicated figures, 50 μm. * p<0.05, ** p<0.01, *** p < 0.001, **** p<0.0001, ns: no significant difference. Precise P values are provided in Raw Data.

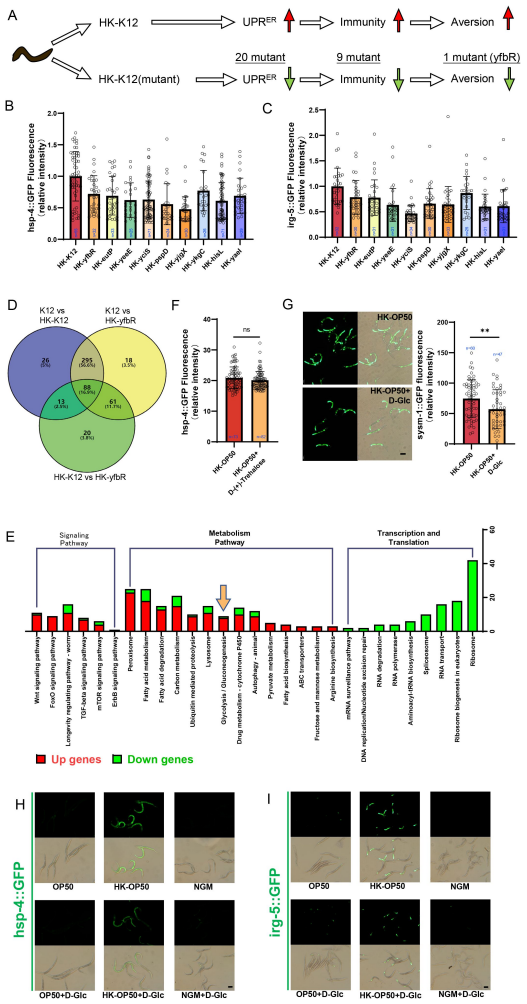

Figure S3.

Low sugar food, HK-*E. coli*, induce stress response and avoidance behavior in animals. Relative to Figure 3.

(A) Flow chart of strategy for *E. coli* keio mutant screening. We identified 20 *E. coli* mutants that did not induce *hsp-4::GFP* through the UPR^{ER} reporter (*irg-5::GFP*) after three rounds of screening (Table S3). From these 20 E. coli mutant, we identified 9 *E. coli* mutants that did not induce *irg-5::GFP* through the immunity reporter (*irg-5::GFP*) screening (Table S3).
(B-C) The bar graph showing that HK-*E. coli* induced *Phsp-4::GFP* (B) and *Pirg-5::GFP* (C) was decreased in animals fed mutant *E. coli* (Heat-killed). n is the number of worms scored from at least three independent experiments. Data are represented as mean ± SD.
(D) Venn diagram showing the number of deferentially metabolites in HK-*E. coli*-K12, HK-*E. coli-yfbR* and *E. coli*.
(E) KEGG enrichment analysis of deferentially expressed genes in animals fed HK-*E. coli* vs live *E. coli*. We noticed that all most of glycolysis/gluconeogenesis genes are up-regulated in animals fed HK-*E. coli*.
(F) The bar graph showing that HK-E. coli induced *Phsp-4::GFP* was not affected in animals with D-(+)-Trehalose supplementation. n is the number of worms scored from at least three independent experiments. Data are represented as mean ± SD.
(G) GFP fluorescence images and bar graph showing that HK-*E. coli* induced *Psysm-1::GFP* was decreased in animals with D-(+)-Glucose (D-Glc) supplementation. n is the number of worms scored from at least three independent experiments. Data are represented as mean ± SD.
(H) UPR^{ER} Reporter (Phsp-4::GFP) expression animals with D-Glc supplementation under OP50, HK-OP50, or NGM condition.
(I) immunity Reporter (Pirg-5::GFP) expression animals with D-Glc supplementation under OP50, HK-OP50, or NGM condition.
For all panels, Scale bar shows on indicated figures, 50 μm. * p<0.05, ** p<0.01, *** p < 0.001, **** p<0.0001, ns: no significant difference. Precise P values are provided in Raw Data.

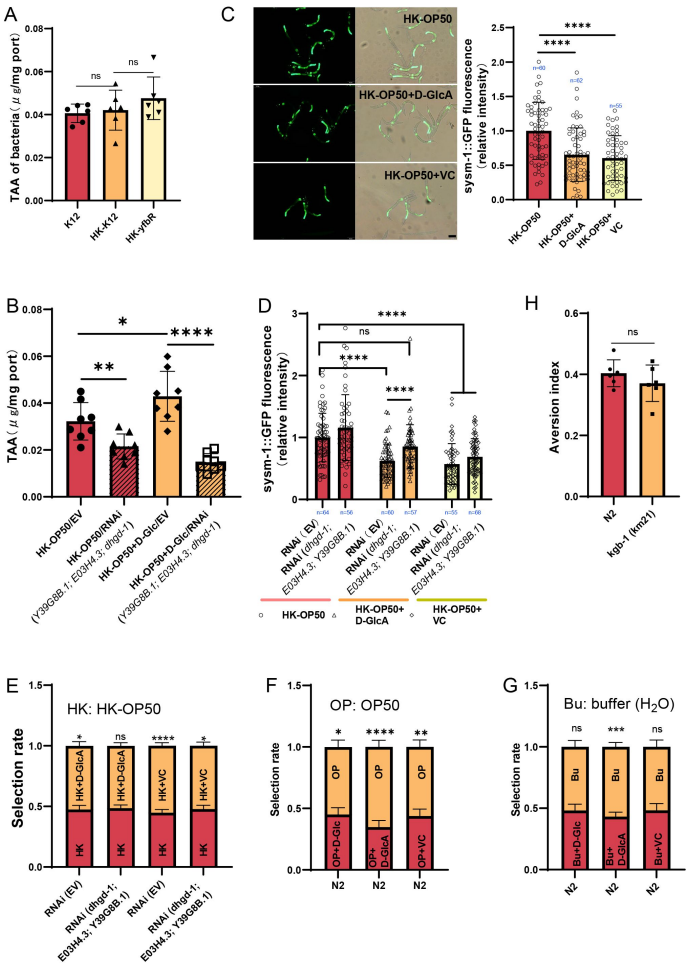

Figure S4.

Vitamin C biosynthesis pathway is critically for evaluating low sugar. Relative to Figure 4.

(A) The level of total L-ascorbic acid (TAA) in Live-K12, HK-K12, or HK-yfbR. N is number of independent experiments. Data are represented as mean ±SD from six independent experiments.
(B) The level of total L-ascorbic acid (TAA) in animals fed HK-*E. coli* with or without D-Glc supplementation. Data are represented as mean ±SD from from eight independent experiments.
(C) GFP fluorescence images and bar graph showing that HK-*E. coli* induced *Psysm-1::GFP* was decreased in animals with D-GlcA or Vitamin C supplementation. n is the number of worms scored from at least three independent experiments. Data are represented as mean ± SD.
(D) The bar graph showing that suppression of HK-*E. coli* induced *Psysm-1::GFP* by D-GlcA supplementation was abolished in animals with RNAi of VC biosynthesis genes, which was not affect by Vitamin C supplementation. n is the number of worms scored from at least three independent experiments. Data are represented as mean ±SD.
(E) Food selection assay showing that the preference of HK-*E. coli* with D-GlcA supplementation was abolished in animals by RNAi of Vitamin C biosynthesis genes. Data are represented as mean ±SD from six independent experiments, 427-775 animals/assay.
(F) Food selection assay for OP50 & OP50 + + D-Glc, D-GlcA, or VC, respectively. Data are represented as mean ±SD from five independent experiments, 241-1182 animals/assay.
(G) Food selection assay for buffer & buffer + D-Glc, D-GlcA, or VC, respectively. Data are represented as mean ±SD from five independent experiments, 8-153 animals/assay.
(H) Food avoidance assay for N2 & kgb-1 mutant animals fed with HK-E. coli. Data are represented as mean ±SD from six independent experiments, 348-660 animals/assay.
For all panels, Scale bar shows on indicated figures, 50 μm. * p<0.05, ** p<0.01, *** p < 0.001, **** p<0.0001, ns: no significant difference. Precise P values are provided in Raw Data.

Star Methods

Resource Availability

Lead contact

Further information and requests for reagents may be directed to the Lead contact Bin Qi (qb@yun.edu.cn).

Materials availability

All reagents and strains generated by this study are available through request to the lead contact with a completed Material Transfer Agreement.

Data and code availability

Metabolomics-seq data are accessible in Table S4 RNA-seq data are accessible in Table S5.

This paper does not report original code.

Any additional information required to reanalyze the data reported in this paper is available from the lead contact upon request.

Experimental model and subject details

C. elegans strains and maintenance

Nematode stocks were maintained on nematode growth medium (NGM) plates seeded with bacteria (*E. coli OP50*) at 20°C.

1) The following strains/alleles were obtained from the Caenorhabditis

Genetics Center (CGC) or as indicated:

N2 Bristol (wild type control strain);

AU78: agIs219 [*T24B8.5p::GFP::unc-54 3' UTR + ttx-3p::GFP::unc-54 3' UTR*];

SJ4005: *Phsp-4::GFP(zcIs4)*;

AY101: acIs101 [*F35E12.5p::GFP + rol-6(su1006)*]IG274: frIs7 [*nlp-29p::GFP + col-12p::DsRed*] IV;

SJ17: *xbp-1 (zc12)*; KU25: *pmk-1(km25)*;

AY102: *pmk-1(km25)* IV; acEx102 [*vha-6p::pmk-1::GFP + rol-6(su1006)*];

YNU108: Ex[*Prgef-1::pmk-1::GFP; Podr-1::RFP*][50];

xbp-1(tm2482) [51];

KU21: *kgb-1(km21)*;

AU133: *agIs17 [myo-2p::mCherry + irg-1p::GFP] IV;*

SJ4100: *zcIs13 [hsp-6p::GFP + lin-15(+)]*.

2) The following strains were constructed by this study:

YNU242: *xbp-1(tm2482); pmk-1(km25)* double mutant was constructed by crossing: *xbp-1(tm2482)* with KU25[*pmk-1(km25)*].

YNU240: ylfEx149 [*xbp-1(tm2482); Prgef-1::xbp-1::GFP; Podr-1::RFP*] transgene strain was constructed by injecting plasmid *Prgef-1::xbp-1::GFP* with *Podr-1::RFP* in *xbp-1(tm2482)* background

YNU241: ylfEx150 [*xbp-1(tm2482); Pges-1::xbp-1::GFP; Podr-1::RFP*] transgene strain was constructed by injecting plasmid Pges-1:xbp-1::GFP with *Podr-1::RFP* in *xbp-1(tm2482)* background

Bacterial strains

E. coli-OP50, *E. coli-K12* (BW25113), and *E. coli-K12* mutant were cultured at 37°C in LB medium. A standard overnight cultured bacteria was then spread onto each Nematode growth media (NGM) plate.

Method Details

Generation of transgenes

- 1) To construct the *C. elegans* plasmid for expression of *xbp-1* in neuron, 3057bp promoter of *rgef-1* and genomic DNA of *xbp-1* was inserted into the PPD95.77 vector. DNA plasmid mixture containing *Prgef-1::xbp-1::GFP* (25ng/ul) and *Podr-1p:RFP* (25ng/ul) was injected into the gonads of adult *xbp-1(tm2482)*.
- 2) To construct the *C. elegans* plasmid for expression of *xbp-1* in intestine, 2549 bp promoter of ges-1 and genomic DNA of xbp-1 was inserted into the PPD95.77 vector. DNA plasmid mixture containing *Pges-1:xbp-1::GFP* (25ng/ul) and *Podr-1p:RFP (25ng/ul)* was injected into the gonads of adult *xbp-1(tm2482)*.

Preparation and feeding of worm food

We followed an established protocol [24,25] to prepare heat-killed (HK) *E. coli*. Briefly, a standard OD600=0.5-0.6 of *E. coli* OP50 and *E. coli* K12 grown in LB broth was concentrated to 1/20 vol and was then heat-killed at 80°C for 180 min. About 150ul of the heat-killed bacteria was spread onto each 35mm NGM plate.

Preparation of HK-*E. coli* + carbohydrate or Vitamin C food

1. 100ul of water, 100ul of L-ascorbic acid (dissolved in water at a concentration of 100mg/ml, Sangon Biotech, 100143-0100) or 100 ul of D-Glucuronic acid (dissolved in water at a concentration of 100mg/ml,Adamas, 1102520) was mixed with 500 ul of HK-*E. coli*, then 150ul of the mixture was spread onto 35mm NGM plates.
2. 12.5ul of water or 12.5ul of D-(+)-Glucose (dissolved in water at a concentration of 100mg/ml, Sangon Biotech, A501991-0500) was mixed with 500 ul of HK-*E. coli*, then 150ul of the mixture was spread onto 35mm NGM plates.

Behavioral assay

C. elegans selection assays

For *C.elegans* to have enough space to evaluate food, we add 18ul of the sample onto a 35mm NGM plate. This creates a round lawn with a radius of 0.5mm, which occupies about 8% of the total plate area.

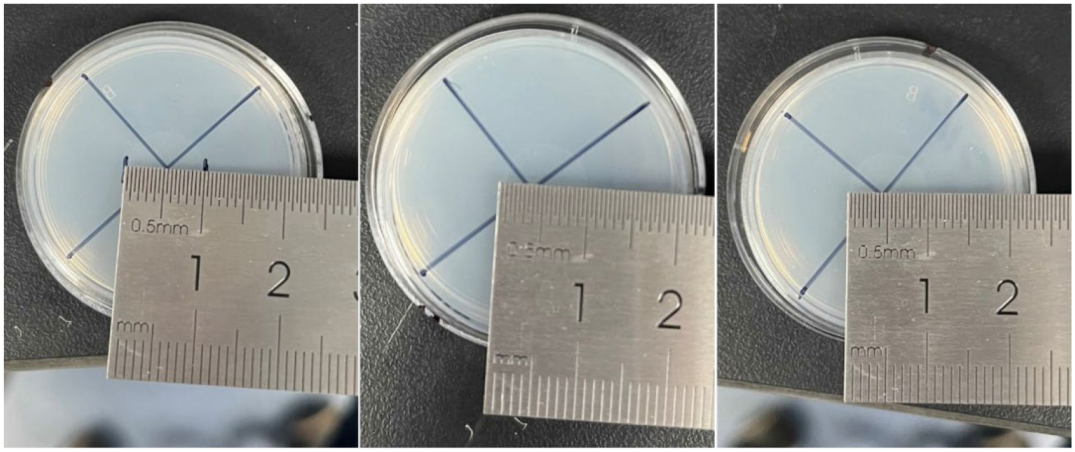

$$\frac{a}{b} = \frac{\pi r_1^2}{\pi \gamma_2^2} = \frac{0.5mm^2}{1.75mm^2} = 8\,\%$$

a: the area of bacterial lawn

b: the space of worm life (area of culture dish)

1. 18ul of heat-killed OP50, live OP50, and LB broth (as the buffer for bacteria) was added into 35mm NGM plate in an equilateral triangle pattern. Then, synchronized L1 worms were seeded in the center of NGM plate for 16-17h at 20°C (as indicated in Figure1B).
2. 18ul of heat-killed OP50 and heat-killed OP50 with D-GlcA or Vitamin C was added into 35mm NGM plate in an equilateral triangle pattern., then synchronized L1 worms were seeded on equilateral triangle of NGM plate for 16-17h at 20°C (as indicated in **Figure 5A**).

Here is Selection rate formula:

$$selection\ rate = \frac{\frac{worm\ amount}{one\ lawn\ area}}{\frac{worm\ amount}{lawn1\ area} + \frac{worm\ amount}{lawn2\ area} + \frac{worm\ amount}{lawn3\ area} \ldots.}$$

C. elegans aversion assays

18ul food was spread out the center of NGM plate, then synchronized L1 worms were seeded on center of food for 16-17h at 20°C.

$$\text{Aversion index} = \frac{worm\ amount\ of\ out\ \text{of}\ lawn}{worm\ amount\ of\ (out + in)\ lawn}$$

Three to ten replicates for each condition were performed for each assay, and the experiments were duplicated on different days.

Analysis of the fluorescence intensity in worms

The synchronized L1 worms carrying either UPR^{ER} reporter (*Phsp-4::GFP*) or innate immunity reporter (*Pirg-5::GFP*; Psysm-1p::GFP; *Pirg-1p::GFP*) were seeded on NGM with indicated food and incubated for 24h at 20 °C. For fluorescence imaging, worms were anesthetized with 25 mM levamisole and photographed using either an Olympus BX53 microscope or Olympus MVX10 dissecting microscope equipped with a DP80 camera.

The fluorescence intensity in entire intestinal region was quantified using ImageJ software and normalized to the body area.

E. coli Keio collection screen

The whole Keio *E. coli* single mutant collection (Baba et al., 2006) was screened. Mutant bacteria strains, as well as the wild-type control strain BW25113, were cultured in LB medium with 50μg/ml kanamycin at 37°Cuntil an OD600 of 0.5-0.6 was reached. The bacteria were then heat-killed following our established protocol [24], and 150 ul of the heat-killed the mutant *E. coli* was spread onto 3.5 cm NGM plates. Synchronized L1 worms carrying UPR^{ER} reporter (*Phsp-4::GPF*) were seeded and cultured for 24h at 20 °C. The fluorescence was then examined by using an Olympus MVX10 dissecting microscope, progressive screening three times. next, an 4^{th} screen was performed using immune reporter (*Pirg-5::GPF*) animals fed with HK-E. coli mutants that reduced the *Phsp-4::GPF* fluorescence. Finally, an aversion behavior assay was performed using HK-*E. coli* mutants that both reduced *Phsp-4::GPF* and *Pirg-5::GPF*. HK-*E. coli* mutants that reduced UPR^{ER}, immune and avoidance behavior were identified through this screening.

RNAi treatment

Bacterial clones from either the MRC RNAi library [52] or the ORF-RNAi Library[53] were used. RNAi plates were prepared by adding IPTG to NGM agar to a final concentration of 1 mM. Overnight *E. coli* cultures (LB broth containing 100 ug/ml ampicillin and 100uM IPTG) of specific RNAi strains and the control HT115 strain were seeded onto RNAi feeding plates and cultured at room temperature until adulthood. Synchronized L1 worms were treated RNAi by feeding (Ahringer, Reverse genetics, WormBook 2006) for the first generation and allowed to grow to maturity. The worms were then bleached and hatched in M9 buffer for 18hr. The synchronized L1 worms were then seeded on the indicated feeding plate.

Western blot

To measure the level of p-PMK-1, worms (feeding different food for 4h) were analyzed by standard western blot methods and probed with anti-p38 (dilution = 1:5,000; Cell Signaling, 9212S), anti-p-p38 (dilution = 1:5,000; Cell Signaling, 4511S) and anti-α-tubulin (dilution = 1:10,000; Sigma T5168) as a loading control.

Total content of ascorbic acid (TAA) assay

The total content of ascorbic acid was measured using the kits (Beijing Biotech-Pack-analytical Scientific Co., Ltd., Beijing, China, BKWB132 *http://biotech-pack-analytical.foodmate.net/*) according to the manufacturer's protocol. Briefly, L1 worms were seeded on the different feeding assay plate and cultured for 4 hours. The worms were then lysed in ice-cold conditions using lysis buffer. Equal amounts of protein were used for the normalization. Here is formula for getting TAA concentration

$$\mathrm{TAA(ug/mg\ prot)} = ((\triangle \mathrm{A} - \mathrm{a}) \div \mathrm{b})) \div (\mathrm{Cpr} \times \mathrm{V1}) \times \mathrm{D}$$

V1 - the volume of supernatant of for experiment

Cpr – the concentration of supernatant protein

D – Dilution ratio of supernatant

a – the intercept of standard curve

b – the slope of standard curve

the standard curve y = 0.0611x + 0.0003 for **Figure 4C**; y = 0.0258x + 0.0066 for **Figure 4B**, **S4A** and **S4B**.

Preparation of samples for RNA sequencing

RNA-seq was done with three biological replicates that were independently generated, collected, and processed. Adult wild type (N2) worms were bleached and then the eggs were incubated in M9 for 18 hours to obtain synchronized L1 worms. L1 worms were cultured in the NGM plate with *HK-E. coli* or *E. coli* for 4hrs at 20°C. L1 worms were then collected for sequencing.

RNA sequencing and data processing

For the RNA sequencing assay, cDNA libraries were constructed, and single-end libraries were sequenced using the Illumina platform (Novogene, Beijing, China). HISAT2 [54] was used to map the clean reads to the reference gene sequence (Species: Caenorhabditis_elegans; Source: NCBI; Reference Genome Version: GCF_000002985.6_WBcel235), and then "featureCounts" tool in subread software [55] was used to calculate the gene expression level of each sample. Read counts were inputted into DESeq2 [56]to calculate differential gene expression and statistical significance. Differentially expressed genes (DEGs) were screened using following criteria: |log2(FoldChange)| > 1 & padj<= 0.05.

Preparation of samples for Metabolome sequencing

Metabolome-seq of bacterial was done with four biological replicates that were independently generated, collected, and processed. Total of three group E. coli sample including: *E. coli K12* (Con), HK-*E. coli K12* (HK), and HK-*E. coli yfbR* mutant (HY). All bacteria were overnight cultured to the same OD (OD600=1). *E. coli K12* and *E. coli yfbR* mutant are heat-killed (80, 180min), *E. coli* K12, HK-*E. coli* K12 and HK-*E. coli yfbR* mutant were then spread out NGM plate for 72hs at room temperature. Finally, sample was collected into 1.5ml tube by using sterile cell scraping.

Metabolome sequencing and data processing

Metabolome were sequenced using the Ultra Performance Liquid Chromatography (UPLC) (ExionLC AD,*https://sciex.com.cn/*) and Quadrupole-Time of Flight (TripleTOF 6600, AB SCIEX) for Non-targeted; Ultra Performance Liquid Chromatography (UPLC) (ExionLC AD, *https://sciex.com.cn/*) and Tandem mass spectrometry (MS/MS) (QTRAP®,*https://sciex.com/*) for Broad targeting (Metware, Wuhan, China). Multiple reaction monitoring (MRM) was used to calculate the expression level of each metabolite. Differential metabolites were screened through Fold change ≥ 2 or Fold change ≤ 0.5 and VIP ≥ 1 (Variable Importance in Projection of OPLS-DA model).

Microscopy

Analysis of fluorescence was performed with an Olympus BX53 microscope or Olympus MVX10 dissecting with a DP80 camera.

Quantification and statistical analysis

Quantification

ImageJ software was used for quantifying fluorescence intensity of UPR^{ER} and Innate immunity reporter. ImageJ software was used for counting the number of worms about selection and aversion behavior.

Statistical analysis

All statistical analyses were preformed using Student's t-test in Graphpad prism 8.0. Two-tailed unpaired t test was used for statistical analysis of two groups of samples. Data are presented as Mean±SD, and $p<0.05$ was considered a significant difference, "*" represents $p<0.05$, "**" represents $p<0.01$, "***" is represents < 0.001, "****" represents $p<0.0001$, "ns" represents no significant difference. For all figures, "n" represents the number of worms scored from at least three independent experiments.

References

1. Filosa A., Barker A.J., Dal Maschio M., Baier H (2016) **Feeding State Modulates Behavioral Choice and Processing of Prey Stimuli in the Zebrafish Tectum** *Neuron* **90**:596–608 https://doi.org/10.1016/j.neuron.2016.03.014

2. Florsheim E.B., Sullivan Z.A., Khoury-Hanold W., Medzhitov R (2021) **Food allergy as a biological food quality control system** *Cell* **184**:1440–1454 https://doi.org/10.1016/j.cell.2020.12.007

3. McLachlan I.G., Kramer T.S., Dua M., DiLoreto E.M., Gomes M.A., Dag U., Srinivasan J., Flavell S.W (2022) **Diverse states and stimuli tune olfactory receptor expression levels to modulate food-seeking behavior** *Elife* **11** https://doi.org/10.7554/eLife.79557

4. Avery J.A., Liu A.G., Ingeholm J.E., Gotts S.J., Martin A (2021) **Viewing images of foods evokes taste quality-specific activity in gustatory insular cortex** *Proc Natl Acad Sci U S A* **118** https://doi.org/10.1073/pnas.2010932118

5. Melin A.D., Nevo O., Shirasu M., Williamson R.E., Garrett E.C., Endo M., Sakurai K., Matsushita Y., Touhara K., Kawamura S (2019) **Fruit scent and observer colour vision shape food-selection strategies in wild capuchin monkeys** *Nat Commun* **10** https://doi.org/10.1038/s41467-019-10250-9

6. Bargmann C.I (2006) **Chemosensation in C. elegans** *WormBook* :1–29 https://doi.org/10.1895/wormbook.1.123.1

7. Sengupta P., Chou J.H., Bargmann C.I (1996) **. odr-10 encodes a seven transmembrane domain olfactory receptor required for responses to the odorant diacetyl** *Cell* **84**:899–909 https://doi.org/10.1016/s0092-8674(00)81068-5

8. Troemel E.R., Kimmel B.E., Bargmann C.I (1997) **Reprogramming chemotaxis responses: sensory neurons define olfactory preferences in C. elegans** *Cell* **91**:161–169 https://doi.org/10.1016/s0092-8674(00)80399-2

9. Fiala A (2007) **Olfaction and olfactory learning in Drosophila: recent progress** *Curr Opin Neurobiol* **17**:720–726 https://doi.org/10.1016/j.conb.2007.11.009

10. Chalasani S.H., Chronis N., Tsunozaki M., Gray J.M., Ramot D., Goodman M.B., Bargmann C.I (2007) **Dissecting a circuit for olfactory behaviour in Caenorhabditis elegans** *Nature* **450**:63–70 https://doi.org/10.1038/nature06292

11. Zhang B., Jun H., Wu J., Liu J., Xu X.Z.S (2021) **Olfactory perception of food abundance regulates dietary restriction-mediated longevity via a brain-to-gut signal** *Nat Aging* **1**:255–268 https://doi.org/10.1038/s43587-021-00039-1

12. Ha H.I., Hendricks M., Shen Y., Gabel C.V., Fang-Yen C., Qin Y., Colon-Ramos D., Shen K., Samuel A.D., Zhang Y (2010) **Functional organization of a neural network for aversive olfactory learning in Caenorhabditis elegans** *Neuron* **68**:1173–1186 https://doi.org/10.1016/j.neuron.2010.11.025

13. Scott K (2018) **Gustatory Processing in Drosophila melanogaster** *Annu Rev Entomol* **63**:15–30 https://doi.org/10.1146/annurev-ento-020117-043331

14. Hukema R.K., Rademakers S., Dekkers M.P., Burghoorn J., Jansen G (2006) **Antagonistic sensory cues generate gustatory plasticity in Caenorhabditis elegans** *Embo J* **25**:312–322 https://doi.org/10.1038/sj.emboj.7600940

15. Ni L., Bronk P., Chang E.C., Lowell A.M., Flam J.O., Panzano V.C., Theobald D.L., Griffith L.C., Garrity P.A (2013) **A gustatory receptor paralogue controls rapid warmth avoidance in Drosophila** *Nature* **500**:580–584 https://doi.org/10.1038/nature12390

16. Jones D., Candido E.P.M (1999) **Feeding is inhibited by sublethal concentrations of toxicants and by heat stress in the nematode Caenorhabditis elegans: Relationship to the cellular stress response** *J Exp Zool* **284**:147–157 https://doi.org/10.1002/(Sici)1097-010x(19990701)284:2<147::Aid-Jez4>3.3.Co;2-Q

17. Xie Z. *et al.* (2022) **The gut-to-brain axis for toxin-induced defensive responses** *Cell* **185**:4298–4316 https://doi.org/10.1016/j.cell.2022.10.001

18. Richardson C.E., Kooistra T., Kim D.H (2010) **An essential role for XBP-1 in host protection against immune activation in C. elegans** *Nature* **463**:1092–U1114 https://doi.org/10.1038/nature08762

19. Kim D.H. *et al.* (2002) **A conserved p38 MAP kinase pathway in Caenorhabditis elegans innate immunity** *Science* **297**:623–626 https://doi.org/10.1126/science.1073759

20. Carr A.C., Maggini S (2017) **Vitamin C and Immune Function** *Nutrients* **9** https://doi.org/10.3390/nu9111211

21. Steinert R.E., Lee Y.K., Sybesma W (2020) **Vitamins for the Gut Microbiome** *Trends Mol Med* **26**:137–140 https://doi.org/10.1016/j.molmed.2019.11.005

22. Li Y., Schellhorn H.E (2007) **New developments and novel therapeutic perspectives for vitamin C** *J Nutr* **137**:2171–2184 https://doi.org/10.1093/jn/137.10.2171

23. Carr A.C., Frei B (1999) **Toward a new recommended dietary allowance for vitamin C based on antioxidant and health effects in humans** *Am J Clin Nutr* **69**:1086–1107 https://doi.org/10.1093/ajcn/69.6.1086

24. Qi B., Kniazeva M., Han M (2017) **A vitamin-B2-sensing mechanism that regulates gut protease activity to impact animal's food behavior and growth** *Elife* **6** https://doi.org/10.7554/eLife.26243

25. Qi B., Han M (2018) **Microbial Siderophore Enterobactin Promotes Mitochondrial Iron Uptake and Development of the Host via Interaction with ATP Synthase** *Cell* **175**:571–582 https://doi.org/10.1016/j.cell.2018.07.032

26. Nakad R. *et al.* (2016) **Contrasting invertebrate immune defense behaviors caused by a single gene, the Caenorhabditis elegans neuropeptide receptor gene npr-1** *BMC Genomics* **17** https://doi.org/10.1186/s12864-016-2603-8

27. Sinha A., Rae R., Iatsenko I., Sommer R.J (2012) **System wide analysis of the evolution of innate immunity in the nematode model species Caenorhabditis elegans and Pristionchus pacificus** *PLoS One* **7** https://doi.org/10.1371/journal.pone.0044255

28. Hetz C., Zhang K., Kaufman R.J (2020) **Mechanisms, regulation and functions of the unfolded protein response** *Nat Rev Mol Cell Biol* **21**:421–438 https://doi.org/10.1038/s41580-020-0250-z

29. Ron D., Walter P (2007) **Signal integration in the endoplasmic reticulum unfolded protein response** *Nat Rev Mol Cell Biol* **8**:519–529 https://doi.org/10.1038/nrm2199

30. Fletcher M., Tillman E.J., Butty V.L., Levine S.S., Kim D.H (2019) **Global transcriptional regulation of innate immunity by ATF-7 in C. elegans** *Plos Genet* **15** https://doi.org/10.1371/journal.pgen.1007830

31. Foster K.J., McEwan D.L., Pukkila-Worley R (2020) **Measurements of Innate Immune Function in C. elegans** *Methods Mol Biol* **2144**:145–160 https://doi.org/10.1007/978-1-0716-0592-9_13

32. Weiss B (2007) **The Deoxycytidine Pathway for Thymidylate Synthesis in Escherichia coli** *Journal of Bacteriology* **189**:7922–7926 https://doi.org/10.1128/jb.00461-07

33. Franceus J., Desmet T (2020) **Sucrose Phosphorylase and Related Enzymes in Glycoside Hydrolase Family 13: Discovery, Application and Engineering** *International Journal of Molecular Sciences* **21** https://doi.org/10.3390/ijms21072526

34. Xing S., Zhang L., Lin H., Mao Z., Bao K., Hao P., Pei Z., Li J., Hu Z (2019) **Lactose induced redox-dependent senescence and activated Nrf2 pathway** *Int J Clin Exp Pathol* **12**:2034–2045

35. Patananan A.N., Budenholzer L.M., Pedraza M.E., Torres E.R., Adler L.N., Clarke S.G (2015) **The invertebrate Caenorhabditis elegans biosynthesizes ascorbate** *Arch Biochem Biophys* **569**:32–44 https://doi.org/10.1016/j.abb.2015.02.002

36. Yabuta Y. *et al.* (2020) **L-Ascorbate Biosynthesis Involves Carbon Skeleton Rearrangement in the Nematode Caenorhabditis elegans** *Metabolites* **10** https://doi.org/10.3390/metabo10080334

37. Moritz B., Schmitz A.E., Rodrigues A.L.S., Dafre A.L., Cunha M.P (2020) **The role of vitamin C in stress-related disorders** *The Journal of Nutritional Biochemistry* **85** https://doi.org/10.1016/j.jnutbio.2020.108459

38. Rice M.E (2000) **Ascorbate regulation and its neuroprotective role in the brain** *Trends in Neurosciences* **23**:209–216 https://doi.org/10.1016/S0166-2236(99)01543-X

39. Webb A.L., Villamor E (2007) **Update: Effects of Antioxidant and Non-Antioxidant Vitamin Supplementation on Immune Function** *Nutrition Reviews* **65**:181–217 https://doi.org/10.1111/j.1753-4887.2007.tb00298.x

40. Maggini S., Wintergerst E.S., Beveridge S., Hornig D.H (2007) **Selected vitamins and trace elements support immune function by strengthening epithelial barriers and cellular and humoral immune responses** *British Journal of Nutrition* **98**:S29–S35 https://doi.org/10.1017/s0007114507832971

41. Luo X., Ng C., He J., Yang M., Luo X., Herbert T.P., Whitehead J.P (2022) **Vitamin C protects against hypoxia, inflammation, and ER stress in primary human preadipocytes and adipocytes** *Molecular and Cellular Endocrinology* **556** https://doi.org/10.1016/j.mce.2022.111740

42. Su M., Liang X., Xu X., Wu X., Yang B (2019) **Hepatoprotective benefits of vitamin C against perfluorooctane sulfonate-induced liver damage in mice through suppressing inflammatory reaction and ER stress** *Environmental Toxicology and Pharmacology* **65**:60–65 https://doi.org/10.1016/j.etap.2018.12.004

43. Ozbey N.P., Thompson M.A., Taylor R.C (2021) **The regulation of animal behavior by cellular stress responses** *Exp Cell Res* **405** https://doi.org/10.1016/j.yexcr.2021.112720

44. Ozbey N.P., Imanikia S., Krueger C., Hardege I., Morud J., Sheng M., Schafer W.R., Casanueva M.O., Taylor R.C (2020) **Tyramine Acts Downstream of Neuronal XBP-1s to Coordinate Inter-tissue UPR(ER) Activation and Behavior in C. elegans** *Dev Cell* **55**:754–770 https://doi.org/10.1016/j.devcel.2020.10.024

45. Troemel E.R., Chu S.W., Reinke V., Lee S.S., Ausubel F.M., Kim D.H (2006) **p38 MAPK regulates expression of immune response genes and contributes to longevity in C. elegans** *Plos Genet* **2** https://doi.org/10.1371/journal.pgen.0020183

46. Mouysset J., Kahler C., Hoppe T (2006) **A conserved role of Caenorhabditis elegans CDC-48 in ER-associated protein degradation** *J Struct Biol* **156**:41–49 https://doi.org/10.1016/j.jsb.2006.02.015

47. Sasagawa Y., Otani M., Higashitani N., Higashitani A., Sato K., Ogura T., Yamanaka K (2009) **Caenorhabditis elegans p97 controls germline-specific sex determination by controlling the TRA-1 level in a CUL-2-dependent manner** *Journal of Cell Science* **122**:3663–3672 https://doi.org/10.1242/jcs.052415

48. Kim K., Li C (2004) **Expression and regulation of an FMRFamide-related neuropeptide gene family in Caenorhabditis elegans** *J Comp Neurol* **475**:540–550 https://doi.org/10.1002/cne.20189

49. Melo J.A., Ruvkun G (2012) **Inactivation of conserved C. elegans genes engages pathogen- and xenobiotic-associated defenses** *Cell* **149**:452–466 https://doi.org/10.1016/j.cell.2012.02.050

50. Geng S. *et al.* (2022) **Gut commensal E. coli outer membrane proteins activate the host food digestive system through neural-immune communication** *Cell Host Microbe* https://doi.org/10.1016/j.chom.2022.08.004

51. Richardson C.E., Kinkel S., Kim D.H (2011) **Physiological IRE-1-XBP-1 and PEK-1 signaling in Caenorhabditis elegans larval development and immunity** *PLoS Genet* **7** https://doi.org/10.1371/journal.pgen.1002391

52. Kamath R.S. *et al.* (2003) **Systematic functional analysis of the Caenorhabditis elegans genome using RNAi** *Nature* **421**:231–237 https://doi.org/10.1038/nature01278

53. Rual J.F. *et al.* (2004) **Toward improving Caenorhabditis elegans phenome mapping with an ORFeome-based RNAi library** *Genome Res* **14**:2162–2168 https://doi.org/10.1101/gr.2505604

54. Mortazavi A., Williams B.A., McCue K., Schaeffer L., Wold B (2008) **Mapping and quantifying mammalian transcriptomes by RNA-Seq** *Nat Methods* **5**:621–628 https://doi.org/10.1038/nmeth.1226

55. Liao Y., Smyth G.K., Shi W (2014) **featureCounts: an efficient general purpose program for assigning sequence reads to genomic features** *Bioinformatics* **30**:923–930 https://doi.org/10.1093/bioinformatics/btt656

56. Love M.I., Huber W., Anders S (2014) **Moderated estimation of fold change and dispersion for RNA-seq data with DESeq2** *Genome Biol* **15** https://doi.org/10.1186/s13059-014-0550-8

Article and author information

Pengfei Liu
Center for Life Sciences, School of Life Sciences, Yunnan Key Laboratory of Cell Metabolism and Diseases, State Key Laboratory of Conservation and Utilization of Bio-resources in Yunnan, Yunnan University, Southwest United Graduate School, Kunming, China

Xinyi Liu
Center for Life Sciences, School of Life Sciences, Yunnan Key Laboratory of Cell Metabolism and Diseases, State Key Laboratory of Conservation and Utilization of Bio-resources in Yunnan, Yunnan University, Southwest United Graduate School, Kunming, China

Bin Qi
Center for Life Sciences, School of Life Sciences, Yunnan Key Laboratory of Cell Metabolism and Diseases, State Key Laboratory of Conservation and Utilization of Bio-resources in Yunnan, Yunnan University, Southwest United Graduate School, Kunming, China
For correspondence: qb@ynu.edu.cn
ORCID iD: 0000-0003-2261-1550

Copyright

Editors

Reviewing Editor
Martin Denzel
Altos Labs, Cambridge, United Kingdom

Senior Editor
Wendy Garrett
Harvard T.H. Chan School of Public Health, Boston, United States of America

Reviewer #1 (Public Review):

Summary:
This manuscript by Liu et al explores the role of the UPR and immune regulators in the evaluation of nutritional quality in C. elegans. They identify neuronal UPR activation and the MAPK PMK-1 as key responders to low food quality. In particular, the data suggest that these

pathways are activated by low levels of vitamin C synthesis that result from the low sugar levels present in heat-killed E. coli.

Strengths:
The results are intriguing and expand our understanding both of physiological food evaluation systems, and of the known roles of stress response pathways in organismal physiology. The authors use a range of techniques, encompassing imaging, metabolomic analysis, gene expression analysis, and behavioural assays, to support their claims.

Weaknesses:
There is limited mechanistic analysis in the study. In particular, how does low vitamin C trigger UPR activation? This is an intriguing finding that, if followed up, could potentially reveal a novel mechanism of UPR activation. In addition, how is the activation of the PMK-1 pathway driven by/coordinated with UPR activation? The data in some figures is not as convincing as it could be: the magnitude of the effect size is small in the supplementation experiments, and the statistical tests used are not always appropriate to enable multiple comparisons.

https://doi.org/10.7554/eLife.94181.1.sa2

Reviewer #2 (Public Review):

Summary:
In this work, the authors aim to better understand how C. elegans detects and responds to heat-killed (HK) E. coli, a low-quality food. They find that HK food activates two canonical stress pathways, ER-UPR, and innate immunity, in the nervous system to promote food aversion. Through the creative use of E. coli genetics and metabolomics, the authors provide evidence that the altered carbohydrate content of HK food is the trigger for the activation of these stress responses and that supplementation of HK food with sugars (or their biosynthetic product, vitamin C), reduces stress pathway induction and food avoidance. This work makes a valuable addition to the literature on metabolite detection as a mechanism for the evaluation of nutritional value; it also provides some new insight into the physiologically relevant roles of well-known stress pathways in modulating behavior.

Strengths:
-The work addresses an important question by focusing on understanding how the nervous system evaluates food quality and couples this with behavioral change.
-The work takes full advantage of the tools available in this powerful system and builds on extensive previous studies on feeding behavior and stress responses in C. elegans.
-Creative use of E. coli genetics and metabolite profiling enabled the identification of carbohydrate metabolism as a candidate source of food-quality signals.
-For the most part, the studies are rigorous and logically designed, providing good support for the authors' model.

Weaknesses:
-It is not clear how the mechanism identified here is connected to previously described, related processes. In particular, it is not clear whether this mechanism has a role in the detection of other low-quality foods. Further, the specificity of the ability of sugar/vitamin C to suppress stress pathway induction is unclear (i.e., does sugar/vitamin C have any effect on the activation of these pathways through other means?). Additionally, the relationship of this pathway to the vitamin B2-sensing mechanism previously described by the senior author is unclear. These issues do not weaken confidence in the authors' conclusions, but they do reduce the potential significance of the work.

-The authors claim that the induction of the innate immune pathway reporter irg-5::GFP is "abolished" in pmk-1(RNAi) animals, but Figure S2K seems to show a clear GFP signal when these animals are fed HK-OP50. Similarly, the claim that feeding WT animals HK-OP50 enriches phospho-PMK-1 levels (Fig 2E) is unconvincing - only one western blot is shown, with no quantification, and there is a smear in the critical first lane.

-The rationales for some of the paper's hypotheses could be improved. For example, the rationale for screening the E. coli mutant library is that some mutants, when heat-killed, may be missing a metabolite that induces the ER-UPR. A more straightforward hypothesis might be that some mutant E. coli strains aberrantly induce the ER-UPR when *not* heat-killed, because they are missing a metabolite that prevents stress pathway induction. This is not in itself a major concern, but it would be useful for the authors to provide a rationale for their hypothesis.

-The authors do not provide any explanation for some unexpected results from the E. coli screen. Earlier in the paper, the authors found that innate immune signaling is downstream of ER-UPR activation. However, of the 20 E. coli mutants that, when heat-killed, "did not induce... the UPR-ER reporter," 9 of them still activate the innate immune response. This seems at odds with the authors' simple model since it suggests that low-quality food can induce innate immune signaling independently of the ER-UPR. Further, only one of the 9 has an effect on behavior, even though failure to activate the innate immune pathway might be expected to lead to a behavioral defect in all of these.

-In a number of places, the writing style can make the authors' arguments difficult to follow.

-Some of the effect sizes observed by the authors are exceedingly small (e.g, the suppression of hsp-4::gfp induction by sugar supplementation in Figs 3C-E), raising some concern about the biological significance of the effect.

-In some cases, there is a discrepancy between the fluorescence images and their quantitation (e.g., Figure 3E, where the effect of glucose on GFP fluorescence seems much stronger in the image than in the graph).

https://doi.org/10.7554/eLife.94181.1.sa1

Reviewer #3 (Public Review):

Summary:
Animals can evaluate food quality in many ways. In contrast to the rapid sensory evaluation with smell and taste, the mechanism of slow nutrient sensation and its impact on food choice is unexplored. The authors utilize C. elegans larvae and their bacterial food as an elegant model to tackle this question and reveal the detailed molecular mechanism to avoid nutrient-poor foods.

Strengths:
The strength of this study is that they identified the molecular identities of the critical players in bacterial food and C. elegans using unbiased approaches, namely metabolome analysis, E. coli mutant screening, and RNA sequencing. Furthermore, they strengthen their findings by thorough experiments combining multiple methods such as genetics, fluorescent reporter analysis, and Western blot.

Weaknesses:
The major caveat of this study is the reporter genes. The transcriptional reporters were used to monitor the UPRER and immune responses in the intestine of C. elegans. However, their

tissue-specific rescue experiments suggest that the genes in the UPRER and immune response function in the neurons. Thus, we should carefully interpret the results of the reporter genes.

Overall, this work provides convincing data to support their model. In the C. elegans field, the behaviors of larvae are not well studied compared to adults. This work will pose an interesting question about the difference between larvae and adults in nutrition sensing in C. elegans and provide a framework and candidate molecules to be studied in other organisms.

https://doi.org/10.7554/eLife.94181.1.sa0